On the origins of transient thermal deformation of concrete

Florent Manzoni, Thierry Vidal, Alain Sellier, Xavier Bourbon, Guillaume Camps

On the origins of Transient Thermal Deformation of Concrete

Florent Manzoni[1], Thierry Vidal[1*], Alain Sellier[1], Xavier Bourbon[2], Guillaume Camps[2]

[1]*LMDC, Université de Toulouse, INSA/UPS Génie Civil, 135 Avenue de Rangueil, 31077 Toulouse cedex 04 France*
[2]*Agence Nationale pour la gestion des Déchets Radioactifs ; Direction Scientifique/Services Colis – Matériaux ; Parc de la croix Blanche 1-7, rue Jean Monnet ; 92 298 Châtenay - Malabry Cedex, France*

* Corresponding author
E-mail address: vidal@insa-toulouse.fr

Keywords: concrete; creep; modelling; temperature; transient thermal deformation

Abstract

The conditions that lead to Transient Thermal Deformation (TTD) of concrete subjected to various temperatures and compressive loads in sealed conditions are analysed and a model based on a two-scale porosity is proposed. In this model, water expands in the smaller pores and diffuses progressively to the capillary pores at the upper scale. It is then shown that the water overpressure in smaller pores and the duration of the diffusion process between the two scales of porosity control the TTD. It is also shown that creep or shrinkage before the temperature transition mitigates TTD. The aim is to provide a model able to predict the conditions for TTD to appear and the amplitude of the TTD under various thermo-mechanical conditions. The TTD model is implemented in an existing basic creep model, fitted and compared with different experimental results.

I. Introduction

In the framework of research surveys steered by the French agency for nuclear waste management (Andra) and the Laboratoire Matériaux et Durabilité des Constructions (LMDC) of Toulouse University, the effect of thermo-hydro-mechanical conditions on concrete deformations have been studied in order to predict the long-term behaviour of High

Performance Concrete (HPC). As nuclear wastes are exothermic, they could induce a rise in temperature (up to a maximum of 50 °C) and a dilation of concrete containment structures which, in return, could lead to a soil reaction and then a loading of the tunnel during the temperature rise. Concomitance of this temperature rise and mechanical loading are favourable to the appearance of Transient Thermal Deformation (TTD) of concrete, so the phenomenon has to be quantified. The few experimental studies available in the literature for the 20 °C to 100 °C temperature range show that, if concretes are loaded and heated simultaneously, they develop greater deformation than if they are heated first and loaded later [1] [2]. This additional strain, called Transient Thermal Deformation (TTD), has been observed up to 105 °C, which is the threshold temperature for C-S-H dehydration [3] [4] [5] [6]. Above this temperature, these authors consider TTD as dehydration creep attributable to chemical transformation due to the temperature increase, which leads to a rearrangement of the microstructure.

The aims of the present work are to clarify the conditions needed for TTD to exist, to understand the physical mechanism that controls it, and then to propose a model able to improve existing creep models in order to consider the influence of the chronology of the thermo-mechanical conditions. After an overview of experimental evidence concerning transient thermal deformation phenomena, the creep model proposed by Sellier et al. [7] is recalled and is improved so as to take TTD into account. The efficiency of the proposed modelling is tested by comparing numerical results with the experimental data.

II. Experimental evidence

According to available data bases [9] [10], transient thermal deformation is irreversible and, if concrete is subjected to heating/cooling cycles under load, TTD only occurs during heating periods. Cagnon et al. [10] have measured the experimental deformations of a mature concrete

(made with CEM I cement) subjected to two thermo-mechanical conditions: first heated and then loaded and, conversely, first loaded and then heated. Figure 1 presents the strain evolutions for the two thermo-mechanical conditions. Contraction is conventionally considered as a negative deformation. The concrete heated first and loaded one day later (blue curves) does not develop TTD, unlike the concrete loaded first then heated one day later (green curves) which does develop TTD. This comparison has shown that the TTD component does not modify the long-term creep kinetics but is just a temporary acceleration of creep. These observations are in accordance with the model of transient thermal creep proposed by Bažant and Kaplan [15]. However, in their model, transient thermal creep can reappear at each temperature variation while the concrete is loaded. Experiments performed by Cagnon did not confirm this aspect, as shown in Figure 1. During the second heating cycle under loading, the two strain evolutions are similar, revealing that TTD does not reappear after the first heating.

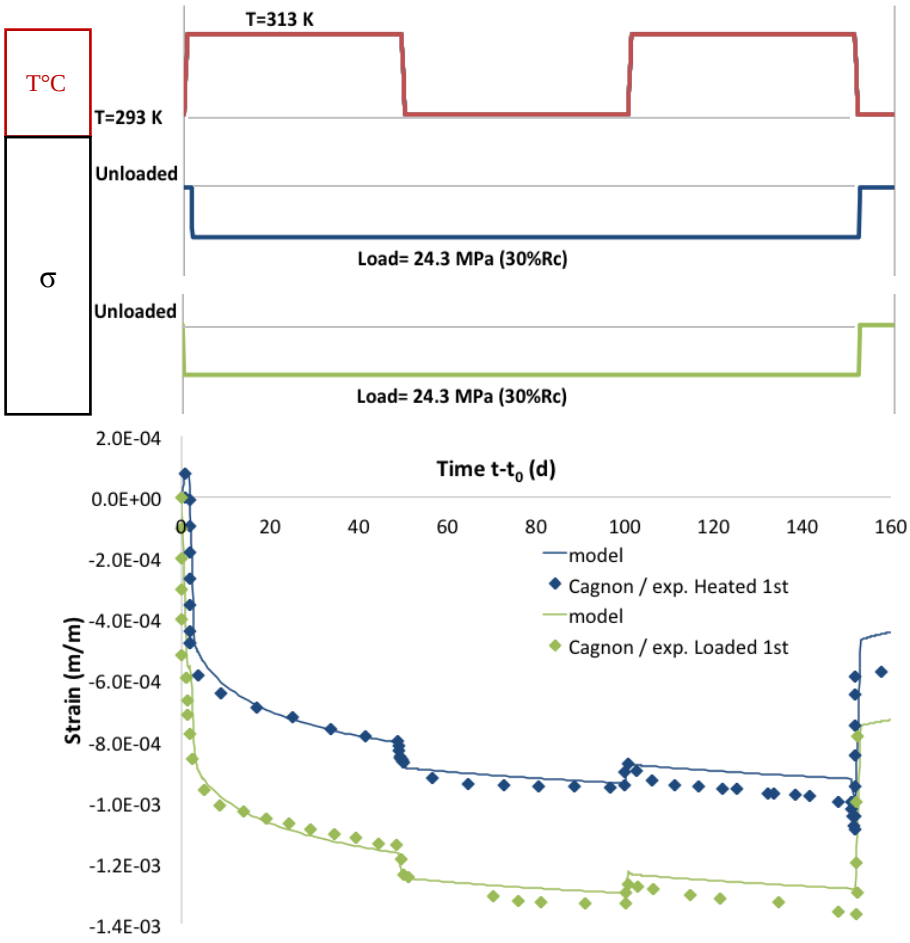

Figure 1: 1st thermo-mechanical conditions: elastic strain, basic creep, thermal dilation and TTD for a sample loaded first (plotted in green) and a sample heated first (plotted in blue), with modelling. t_0 corresponds to the end of water curing and R_c is the compressive strength (experimental results from [10])

This non-repeatability in case of heating is one of the main points of discussion. For several authors [5] [10] [11], TTD appears only once, with the first heating, and it can reappear only if the temperature peak reached in previous heating is exceeded. Fahmi et al. [9] showed that saturated concrete developed TTD even after several cycles of heating/cooling. However, for concrete stored at 50% RH, this repeatability did not exist. Thus, he showed that the water content modified the amplitude of the TTD. This strain dependence on the degree of saturation has been confirmed by Cagnon et al. [10] and Hansen and Eriksson [12]. Moreover, the loading rate and heating kinetics can also influence TTD [1].

To explain this phenomenon, various assumptions have been proposed. According to Khoury and Parrot [11] [13], the origin of TTD could be a differential thermal dilation between the

various concrete phases and the associated microcracking. However, TTD is also observable on cement paste, so its origin cannot be attributed only to the differential thermal dilation between paste and aggregates. Torrenti [14] proposed a damage model coupled with creep to simulate the transient thermal deformation. In his model, the evolution of damage amplifies the stress and thus the viscoelastic strain; the additional strain obtained is considered to be the TTD. Experimentally, the evolution of Young's modulus measured before and after thermo-mechanical tests at 40 °C in [10] showed that TTD did not damage the material. Several authors suggest that the transient thermal deformation phenomenon has its origin in water movement at the nanoporous C-S-H scale [10] [12] [15] [16] [17]. Some models proposed are usually based on self-desiccation [15] or thermal activation [6] [18] [19] and are a function of the thermal variation rate ($\dot{T}$). Thus, according to these models, the transient thermal strains will be repeated in case of heating cycles, whatever the maximum temperature reached, which is not in accordance with Cagnon's experimental observations. Thus, there is a need to improve the understanding and the modelling of this phenomenon. For this purpose, a double-scale porosity model with water transfer from one scale to the other is proposed. The overpressure in the finest porosity is assumed to control the material viscosity. This dependence of the viscosity on the pressure at nanoscale is implemented in an existing basic creep model and successfully confronted with literature results.

III. Modelling of experiments

This section first presents the creep model in which the TTD is to be implemented. A lot of creep models are proposed in the literature. Benboudjema et al. [20] split the basic creep into a spherical and a deviatoric part. Thus de spherical creep corresponding to a migration of adsorbed water in micro and nanoporosity and the deviatoric creep is the sliding of C-S-H layers. The model is based on the assumption that the basic creep kinetics of concrete is controlled by two antagonistic phenomena: the material viscosity, which allows creep, and a

consolidation phenomenon, which corresponds to a transfer of stresses from viscous particles (typically C-S-H bundles) to elastic particles (other hydrates and aggregates). As the stresses in the non-viscous particles increase, the C-S-H are unloaded, which slows down their strain rates. TTD is assumed to take place in the nanoporisity of C-S-H bundles: due to the temperature rise, the embedded water dilates and its pressure increases, transiently modifying the bond between C-S-H particles and so their viscosity. Once this overpressure has been depleted by diffusion of water from the C-S-H to capillary pores, the C-S-H bundles return to their initial configurations and the creep velocity returns to that of basic creep.

III.1. Principles of the creep model

The model chosen to implement the TTD phenomenon is described in [7]. As explained above, in this model the slowdown of creep kinetics is due to a consolidation phenomenon that increases the apparent material viscosity. The consolidation function assumes that there is a strain potential that is intrinsic to the concrete, and each deformation (shrinkage and creep) consumes this potential and consolidates the material, thus slowing down creep. The strain is modelled with a Maxwell model in which the viscosity evolves with the strain [7]; this strain corresponds to ε^{MC} in Eq. (1).

Meanwhile, Cagnon et al. [10] observed experimentally that TTD did not modify later creep kinetics. In other words, the creep kinetics is the same at the end of the TTD whatever the TTD magnitude. Everything happens as if the concrete fluidifies momentarily, without any effect of TTD on the consolidation process. From a macroscopic point of view, this is similar to a temporary fluidification of concrete that disappears approximately with the end of heating. As basic creep and TTD are both viscous strains but only the basic creep creates a consolidation, the creep strain ε^{M} in Eq. (1) has be decomposed into two parts: a consolidating strain ε^{MC} (corresponding to the initial basic creep model proposed in [7]) and

an un-consolidating strain $\varepsilon^{M\bar{C}}$ for the TTD. The former corresponds to the basic creep, which depends and acts on the consolidation process, and the latter, corresponding to the TTD, depends on the consolidation but does not act on it.

$$\frac{\partial \varepsilon^{M}}{\partial t} = \frac{\partial \varepsilon^{MC}}{\partial t} + \frac{\partial \varepsilon^{M\bar{C}}}{\partial t} \quad (1)$$

The two components of this creep model are explained below: first the basic creep part, then the TTD.

III.2. Basic creep equations

The strain ε^{MC} corresponding to basic creep comes from Sellier et al. [7]. It is briefly recalled in this part.

III.2.1. Permanent creep

In each main direction, $_I$, of elastic strain, the basic creep velocity, presented in Eq. (2), is proportional to the elastic strain ε_I^E *via* a characteristic time τ_I^M:

$$\frac{\partial \varepsilon_I^{MC}}{\partial t} = \frac{\varepsilon_I^E}{\tau_I^M} . C^w \quad (2)$$

In Eq. (2), C^w stands for the influence of water content on creep velocity. It is given by Eq. (3). The temperature acts through the moisture effect because water viscosity changes with temperature [21]. This effect is modelled with an Arrhenius law in Eq. (4). In this equation, E_W^a corresponds to the water viscosity activation energy (≈17000 J/mol), R is the perfect gas constant (8.31 J/mol/K) and T_{ref} is the reference temperature (for which τ_{ref}^M (Eq. 6) is fitted). As C-S-H properties also depend directly on the water content, the term C_s^w (Eq. 5) is used. It corresponds to the water saturation of the porosity, Sr, and allows creep velocity reduction when the concrete dries.

$$C^w = C_s^w . C_T^w \quad (3)$$

$$C_T^w = exp\left(-\frac{E_W^a}{R}\left(\frac{1}{T}-\frac{1}{T_{ref}}\right)\right) \quad (4)$$

$$C_s^w = Sr \quad (5)$$

The characteristic time τ_I^M of Eq. (2) is defined by Eq. (6) where τ_{ref}^M is a fitting parameter (reference characteristic time) characterizing the initial creep velocity of a saturated concrete never loaded before.

$$\tau_I^M = \tau_{ref}^M . C_I^c \quad (6)$$

C_I^c is the consolidation function. It allows the creep velocity to be modified according to the creep that has already occurred and the thermo-mechanical conditions that are integrated into the creep coefficient k presented in Eq. (8)

$$C_I^c = \frac{1}{k} exp\left(\frac{1}{k}\left(\frac{\varepsilon_I^{MC}}{\varepsilon_I^E}\right)^+\right) \quad (7)$$

The function C_I^c increases with the permanent strains ε_I^{MC} due to shrinkage and creep, expressing a material consolidation. Thus, it induces a function enhancing the characteristic time and leading to a creep velocity decrease.

$$k = k_{ref} . C_p^T . C^M \quad (8)$$

In this equation, C_p^T (Eq. 10) and C^M (Eq. 11) stand for the thermal and the mechanical effects on creep potential, respectively, according to Sellier et al. [7]. C_p^T considers the effect of thermal damage and C^M the effect of mechanical damage. Thus, in case of thermo-mechanical variations, the potential is automatically adapted. k_{ref} is the creep coefficient calculated in Eq. (9). Note that these temperature effects are not the causes of TTD but only the causes of basic creep velocity dependence on the temperature.

$$k_{ref} = \frac{\varepsilon_{ref}^M}{\varepsilon_{ref}^E} \quad (9)$$

ε_{ref}^{M} is a fitting parameter called the reference creep potential, which represents an inherent permanent delayed strain characteristic of the material; ε_{ref}^{E} is the reference elastic strain defined as the material deformation under uniaxial compressive stress of 33% of its compressive strength.

According to Ladaoui et al. [22], the differential dilation between paste and aggregates could cause thermal damage and increase creep potential. This damage is modelled with an Arrhenius law, as presented in Eq. (10).

$$C_p^T = \begin{cases} exp\left(-\frac{E_p^a}{R}\left(\frac{1}{T}-\frac{1}{T_{thr}}\right)\right) & if\ T > T_{thr} \\ 1 & if\ T \le T_{thr} \end{cases} \quad (10)$$

T_{thr} is the threshold temperature (≈45 °C for the material studied in [22]) above which thermal damage occurs, and E_p^a is a fitted activation energy (≈25000 J/mol).

The C^M coefficient takes the possible non-linear effect between creep potential and mechanical loading level into account, through an equivalent Drucker-Prager shear stress τ^{DP}. In Eq. (11), the critical shear stress τ_{cr}^{DP} is the critical value causing tertiary creep by micro-structure damage.

$$C^M = \frac{\tau_{cr}^{DP}}{\tau_{cr}^{DP} - \tau^{DP}} \quad (11)$$

To consider the beneficial effects of triaxial confinement in reducing the impact of deviatoric stress, τ^{DP} is calculated in Eq. (12), which corresponds to a Drucker-Prager criterion:

$$\tau^{DP} = \sqrt{\frac{\sigma^d : \sigma^d}{2}} + \delta\frac{Tr(\sigma)}{3} \quad (12)$$

where σ^d is the deviatoric part of the stress tensor and δ is the confinement effect coefficient. The critical shear stress is linked to a corresponding uniaxial critical compressive stress intensity, σ_{cr}, presented in Eq. (14).

$$\tau_{cr}^{DP} = \frac{\sigma_{cr}}{\sqrt{3}}\left(1 - \frac{\delta}{\sqrt{3}}\right) \quad (13)$$

$$\sigma_{cr} = \frac{2}{3} R_c \left(\frac{\chi^M}{\chi^M - 1}\right) \quad (14)$$

χ^M is a non-linear creep coefficient corresponding to non-linear creep amplification observed under a compression stress of 66% of the compressive strength and is close to 2 for an Ordinary Portland Cement based concrete [7].

III.2.2. Reversible creep

In this model, a reversible creep is modelled using a Kelvin module ε_I^K (Eq. 15). The maximum amplitude of reversible creep is made proportional to the elastic strain by means of parameter ψ^K.

$$\frac{\partial \varepsilon_I^K}{\partial t} = \frac{1}{\tau^K}\left(\frac{\varepsilon_I^E}{\psi^K} - \varepsilon_I^K\right) \quad (15)$$

The characteristic time τ^K is defined by Eq. (16), where τ_{ref}^K is a fitting parameter associated with a reference time characterizing the initial material recovery.

$$\tau^K = \tau_{ref}^K . C_T^w \quad (16)$$

A thermal effect parameter C_T^w affects the reversible creep velocity in the same way as for the permanent creep Eq. (4).

III.3. Modelling of Transient Thermal Deformation

The strain associated with the TTD is $\varepsilon^{M\bar{C}}$ in Eq. (1). It is now presented and explained.

III.3.1. Physical phenomenon

According to Vlahinić et al. [23], transient creep under moisture content variation can be modelled by a modification of the material viscosity in relation to the fluid interflow at nanoscale. This flow is activated to balance a pressure difference between two pore regions, macropores and nanopores. In our case, if the material is heated, nanoporous water dilation

changes C-S-H organization and consequently modifies their apparent viscosity until the overpressure induced by the water dilation is depleted by the flow from C-S-H intra porosity to the capillary porosity at the upper scale. During this process, the C-S-H viscosity is reduced and the phenomenon can be considered as a transient fluidification of concrete, which causes creep amplification. The pressure difference between capillary and nanoporosity causes water to diffuse from nanopores to capillary pores until the pressures rebalance. Consequently, if the material is heated long enough before mechanical loading, the water transfer is finished before the creep strain develops and TTD does not occur. Thus, the transient thermal deformation can appear only if the loading is applied before the fluidification is over and thus before the system has returned to a steady state.

III.3.2. Water transport equation

To model the nanoporous pressure P^n in C-S-H bundles, a poro-mechanics analogy is proposed (Eq. 17).

$$P^n = M^n\left(\emptyset^n - \emptyset^n_{ref}\right) \qquad (17)$$

For a unit volume of concrete, the water pressure P^n is proportional to the difference between the C-S-H nanoporous water volume, $\emptyset^n$, and to a reference volume, $\emptyset^n_{ref}$. At this scale, the porosity is an adsorbed layer that stays saturated with water even if the hygrometry is low (down to 11% RH) according to Jennings [24]. Thus, $\emptyset^n_{ref}$ can also be considered equivalent to the initial nanoporous volume of C-S-H. The C-S-H gel represents approximately 70% of the cement paste volume for classical cementitious material (Portland cement), and the average porosity is 28% [26]. According to Jennings [27], the nanoporosity of C-S-H is of the order of 18% of the global porosity. Consequently, the nanoporous volume is roughly 3.5% of the cement paste volume (0.7x0.28x0.18 = 0.035m^3/m^3 of cement paste). The proportionality coefficient M^n is also defined in the framework of the poro-mechanics analogy, through Eq.

(18). It is a Biot modulus at the C-S-H scale, which considers the interactions between C-S-H and water.

$$\frac{1}{M^n} = \frac{b^n - \emptyset^n_{ref}}{K^r} + \frac{\emptyset^n_{ref}}{K^w} \quad (18)$$

where b^n is the Biot coefficient for nano sites (≈ 0.65) [25]; K^r is the C-S-H stiffness; K^w is the water compressibility, which can be considered as a constant in the temperature range studied (≈ 2 300MPa). Under the assumption that C-S-H stiffness is about 30 GPa [28], the Biot modulus is approximately 28 GPa.

The flow necessary to rebalance the pressure difference between nanoscale and capillary scale is defined through Eq. (19) for a unit of material volume. The pressure difference is dissipated by water diffusion until the system is balanced, i.e. $P^n = P^c$.

$$\frac{\partial m^{n\to c}}{\partial t} = -\frac{k^n.(P^n - P^c)}{\eta(T)}.\rho(T) \quad (19)$$

In this equation, the mass flow $\frac{\partial m^{n\to c}}{\partial t}$ from the nanoporous to capillary scale depends on the water nanoporous pressure P^n, water capillary pressure P^c, fluid apparent viscosity η and fluid density ρ, which depend on the temperature. A fitting parameter k^n is introduced to control the flow velocity. This parameter can be considered as a dimensionless coefficient of permeability at nanoscale. Its value can vary because the morphologies of C-S-H change according to the concrete formulation (high density or low density C-S-H for instance). At the capillary scale, the water capillary pressure, Eq. (20), is obtained from the Van-Genuchten isotherm, without the gas pressure, according to the assumption proposed by Mensi et al. [29] and presented as a function of capillary saturation state Sr^c.

$$P^c = -M^c(T).\left(Sr^{c\left(-\frac{1}{mvg}\right)} - 1\right)^{(1-mvg)} \quad (20)$$

mvg is the fitting parameter controlling the shape of the isotherm curve, and M^c is a fitting parameter proportional to the capillary tension (Eq. 21), and thus depending on the temperature in order to respect an isothermal model with temperature variation (Figure 2) as proposed by Chhun [30].

$$M^c(T) = M^{c,ref}\left[exp\left(-\frac{T-T_{ref}}{\Delta T_{ref}}\right)\right] \quad (21)$$

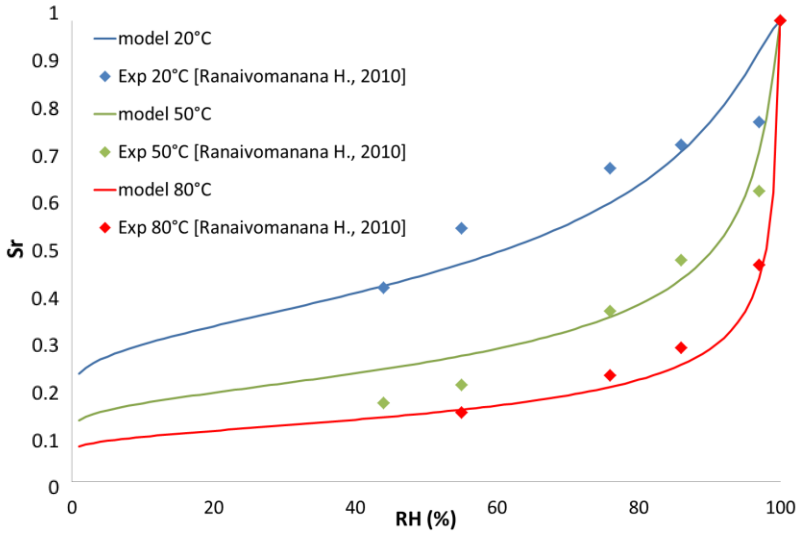

Figure 2: Modelling of desorption isotherms at different temperatures [30]

In this equation, $M^{c,ref}$ is the capillary tension coefficient at the reference temperature, T_{ref}, and ΔT_{ref} is a reference temperature variation presented in Table 1. The capillary tension, and consequently the water capillary pressure, decrease when heating is applied.

Constants	Value used
ΔT_{ref}	20 K
T_{ref}	293 K
$M^{c,ref}$	10 MPa
mvg	0.26

Table 1: Values of constants used to model the capillary tension [30]

The effect of temperature, T, on water density, ρ, is modelled using the empirical equation proposed by Thiensen, Eq. (22) [31].

$$\rho(T) = \rho^{ref}.\left[1 - \frac{(T-T_1)^2.(T-T_2)}{{T_3}^2.(T-T_4)}\right] \quad (22)$$

ρ^{ref} is the reference water density at 273 K and at atmospheric pressure; the other parameters are presented in Table 2. The water density decreases with heating as represented in Figure 3 within the studied temperature range.

Constant	Value used for water
T_1	269.017 K
T_2	574.797 K
T_3	722.86 K
T_4	342.349 K
ρ^{ref}	999.975 kg/m^3

Table 2: Values of constants in Thiensen equation

Ladaoui et al. [21] model the water viscosity evolution with temperature, Eq. (23), with an Arrhenius law as the C_T^w coefficient of Eq. (4):

$$\eta(T) = \frac{\eta^{ref}}{e^{-\frac{E_W{}^a}{R}\left(\frac{1}{T}-\frac{1}{T^{v,ref}}\right)}} \quad (23)$$

This law is a function of a reference viscosity η^{ref} (2.07x10^{-14} MPa.d) at a reference temperature $T^{v,ref}$ (273 K). The evolution of the viscosity is presented in Figure 3. It decreases with temperature rise, which facilitates the C-S-H movement by lubrication.

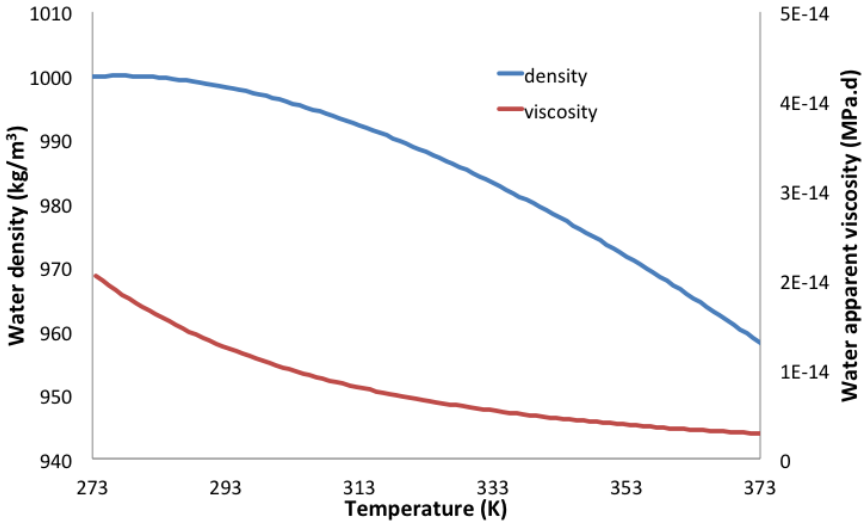

Figure 3: Modelling of water density and apparent viscosity evolution versus temperature [31] and [21].

Considering the small quantity of water exchangeable between nanoscale and capillary scale, the water supplied to the capillary porosity is assumed not to affect the capillary pressure, which is mainly controlled by the water exchanges at capillary scale only.

The introduction of the nanoporous water pressure (Eq. 17) in the diffusion equation (Eq. 19) links the capillarity pressure and the nanoporous water pressure (Eq. 24).

$$\frac{\partial P^n}{\partial t} = \frac{(P^c - P^n)}{\tau^n} \qquad (24)$$

with τ^n the characteristic time for the evacuation of nanoporous pressure defined in Eq. (25).

$$\tau^n = \frac{\eta(T)}{M^n.k^n}. \qquad (25)$$

Therefore, the state variable of this physical phenomenon is simply the C-S-H nanoporous water pressure.

Figure 4 illustrates the pressure evolution of nanoporous water modelled with the parameter values (Table 4) used to fit Cagnon's experimental data [10] (Figure 1 and Figure 7). When the temperature rises, the water thermal dilation creates an overpressure in nanoporosity until the temperature stabilizes. From that moment, water diffusion allows the nanoporous water pressure to decrease until it returns to equilibrium with the capillary pressure. When cooling, the nanoporosity is in depression and the water diffuses from the capillary to the nanoporous volume. If the material is heated quickly, the water in the nanopores does not have enough time to be evacuated and the pressure is amplified.

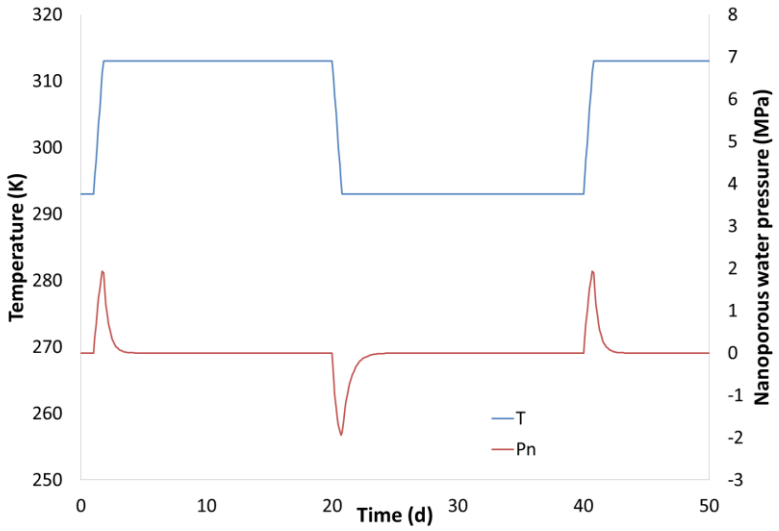

Figure 4: Example of water nanoporous pressure evolution under temperature cycle (20-40-20 °C) with k^n=7.16x10^{-19} and P^c=0 MPa.

III.3.3. Evolution of transient thermal deformation

As for basic creep (Eq. 2), the transient thermal deformation is assumed proportional to the elastic strain ε_I^E, Eq. (26).

$$\frac{\partial \varepsilon^{M\bar{C}}}{\partial t} = \frac{\varepsilon_I^E}{\tau_I^M} . C_n^w \qquad (26)$$

The Maxwell characteristic time τ_I^M presented in Eq. (26) is the same as in Eq. (6), but it is affected by the coefficient C_n^w used to model the influence of nanoporous water pressure on the C-S-H viscous behaviour. This coefficient has to make a temporary decrease of the material viscosity possible as long as the nanopressure is not depleted, which induces an equation of the form (27):

$$C_n^w = \begin{cases} \frac{P^n}{P_k^n} & if\ P^n > 0 \\ 0 & if\ P^n \leq 0 \end{cases} \qquad (27)$$

If the C-S-H intra porosity is in depression or at equilibrium with respect to the water capillarity ($P^n = P^c$), C_n^w is equal to zero, which means that TTD does not occur. But, in case of nanoporous overpressure, a linear relation between C_n^w and P^n controls the TTD kinetics through the fitting parameter P_k^n (which has the dimension of a pressure). Thus, if a saturated, mechanically loaded material is subjected to heating, an overpressure appears and leads to

TTD. Over time, the nanoporous pressure decreases to balance the capillary pressure, slowing the TTD kinetics.

In Figure 5, the maximum TTD velocity is reached at the maximum temperature and decreases quickly until falling to zero just a few hours later (due to water diffusion). With these equations, if a concrete is heated a long time after its mechanical loading, the TTD is lower than if it was heated just after its mechanical loading. Before the rise in temperature, the shrinkage and creep of concrete will increase the consolidation (and so the characteristic time τ_I^M), and consequently decrease the TTD velocity according to Eq. (26).

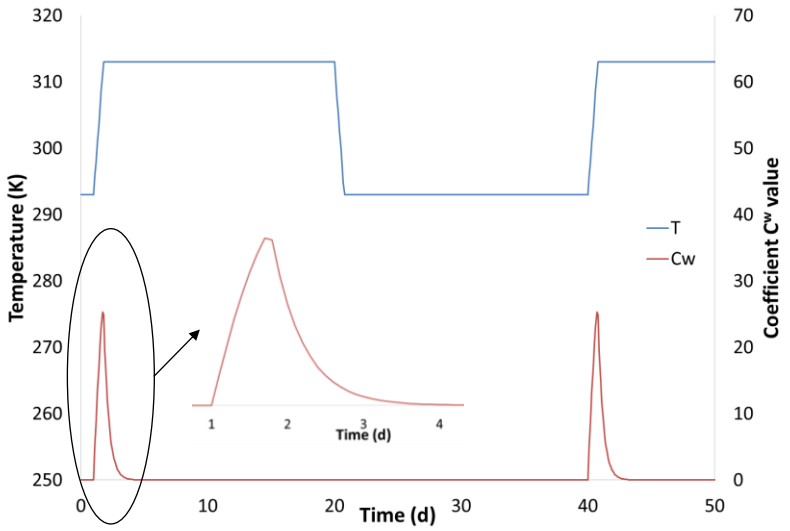

Figure 5: Example of evolution of moisture coefficient C_n^w with time under temperature cycle T (20-40-20°C) with k^n=7.16x10^{-19}, P_k^n=102kPa and P^c=0MPa.

As shown by Fahmi et al. [9], for saturated concrete ($P^c = 0\ MPa$), the TTD can be repeated if temperature cycles are close together because the consolidation cannot progress enough to significantly affect the characteristic time of these delayed strains.

IV. Application

The equations introduced previously were tested on experimental results from Cagnon et al. [10]. This part presents the application to sealed samples. The sealing was used to prevent the desiccation of the specimens during the tests. Before the tests, samples were cured in water at

20 °C for more than 3 months after casting to allow their hydration to stabilize, then they were sealed just before thermo-mechanical conditions were applied.

The concrete used was a High Performance Concrete made with CEM I cement. The values of its instantaneous mechanical properties and its coefficient of thermal expansion are presented in Table 3. The experimental and calculated strains were obtained on uniaxial compressive loading at 24.3 MPa. To model the TTD, the creep parameters were required, thus basic creep was also modelled.

	Value
Young's modulus E (GPa)	45.5
Compressive strength (MPa)	82.9
Poisson's coefficient (ν)	0.2
Coefficient of thermal expansion (K^{-1})	4.10^{-6}

Table 3: Concrete properties

The modelling of elastic strain and the basic creep presented in Figure 6 allowed fitting parameters to be determined, which are summed up in Table 4 (τ_{ref}^{M}, τ_{ref}^{K}, ψ^{K} and ε_{ref}^{M}). These parameters were maintained for all the following modelling.

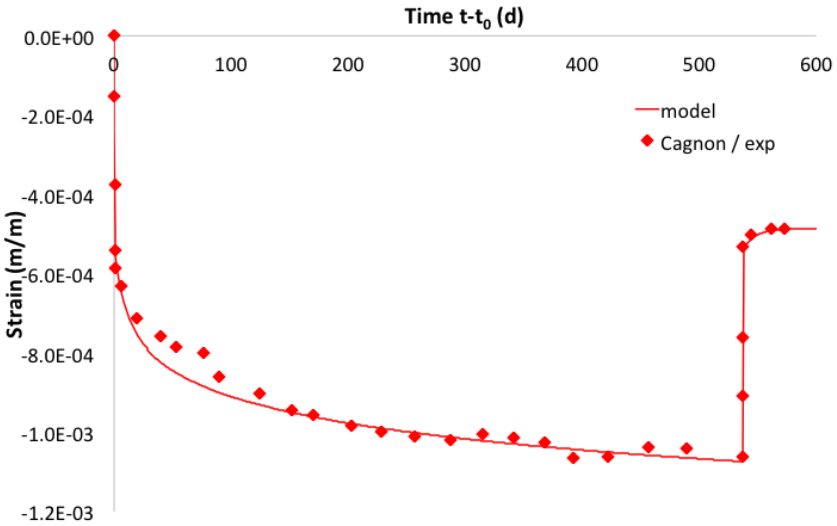

Figure 6: Experimental modelled strain evolutions under loading (30%Rc) versus time from t_0 date of loading at 20°C with instantaneous elastic strain and creep strain (experimental results from [10])

Figure 7 shows the experimental evolutions of strain corresponding to a second set of thermo-mechanical conditions from Cagnon's data, which will be used for modelling. In this test,

sealed concrete was loaded one day before heating and was then subjected to thermo-mechanical variations as detailed above the graph.

In this figure, the model is first used without TTD (black curve), in order to show the underestimation of strain when TTD is not considered. It is obvious that, in this case, the basic creep modelling with thermal activation is not sufficient, and the missing part constitutes the TTD. TTD appears early and its amplitude can be estimated at approximately 300 µm/m. However, it is noteworthy that the velocity of strains after 10 days, computed by the model fitted above, is of the same order as found experimentally. This result shows clearly that TTD is a strain shift that occurs during heating without affecting the consolidation phenomenon responsible for the basic creep curve shape.

When the TTD model is activated, the TTD parameters (k^n and P_k^n) are fitted using a least-squares method. The parameter values are given in Table 4 and the completed model is presented in Figure 7.

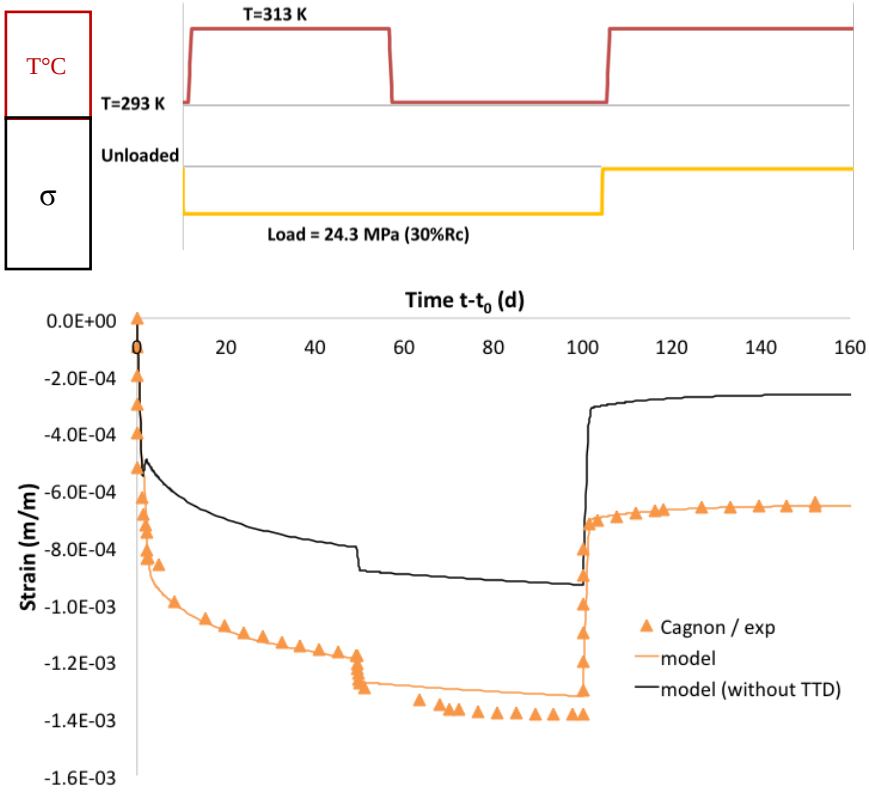

Figure 7: 2nd thermo-mechanical conditions: elastic strain, basic creep, thermal dilation and TTD, with and without TTD modelling (experimental results from [10])

To test the model, the first thermo-mechanical evolution presented in Figure 1 was modelled with the same set of parameters (the result of model fitting is shown in Figure 1). Some samples (plotted in blue, mean value) were heated then loaded and others (plotted in green, mean value) were loaded then heated. From the comparison of model and experimental results, the model was found to be able to predict the measured strain evolution with the same set of parameters if TTD occurred. The effect of consolidation on repeatability of TTD in the case of a heating cycle was also taken into account as shown by the green curve. As expected, TTD appears with the first heating. However, during the second heating, the previous consolidation (due to creep and shrinkage), and consequently the characteristic time τ_I^M, are sufficient to prevent TTD from occurring again. If the thermal cycle had been closer in time, the consolidation would have been less developed and the TTD could have been repeated. This may be especially relevant for saturated concrete, which thus has not been previously consolidated by capillarity tension.

Model parameter	Value
τ_{ref}^{M} (days)	4
τ_{ref}^{K} (days)	10
ψ^{K} (-)	10
ε_{ref}^{M} (-)	$8.8.10^{-5}$
P_k^n (kPa)	102 $7.16.10^{-19}$
k^n (-)	

Table 4: Fitting parameters for concrete creep and transient thermal deformation

Conclusion

Based on experimental observations, the TTD known to occur only if heating occurs after or simultaneously with the mechanical loading is similar, at the macroscopic scale, to a sort of a transient fluidification conditioned by two other phenomena: firstly, the concrete should not have undergone creep before loading and, secondly, the water saturation must be sufficient during the heating. If these four conditions (loading, heating, no or slight creep before heating, high saturation ratio) are fulfilled, then TTD can occur. To model the occurrence and the amplitude of the TTD as simply as possible, it is assumed that the origin of the TTD remains in the nanoporous water of C-S-H. When heated, nanoporous water dilates and changes the C-S-H viscosity until the local overpressure at this scale is depleted by diffusion of this water towards the capillary porosity. The proposed model then allows simulations of various experimental strain evolutions to be performed under several thermo-mechanical conditions with a single set of parameters. This model is sufficiently easy to use to be implemented in a basic creep structural model. This possibility will now allow the risk of TTD to be automatically considered in finite element structural analysis. Despite this modelling, which can determine the occurrence and the amplitude of the phenomenon, determining the physical reasons why the viscosity of C-S-H bundles is so dependent on the water pressure at nanoscale remains a challenge, especially for researchers working on homogenization theory and on modelling at atomic scale.

Acknowledgements

This work was carried out at LMDC (University of Toulouse), in collaboration with and with support from Andra (the French agency for nuclear waste management).

References

[1] Schneider U. (1982), Behavior of concrete at high temperatures, Paris: RILEM-Report to Committee, 72.

[2] Illston J.M., Sanders P.D. (1973), The effect of temperature change upon the creep of mortar under torsional loading, Magazine of Concrete Research 25 (84), 136-44.

[3] Sabeur H., Meftah F. (2008), Dehydration Creep of Concrete at High Temperatures, Materials and Structures 41 (1), 17-30.

[4] Gawin D., Pesavento F., Schrefler B.A. (2004), Modelling of Deformations of High Strength Concrete at Elevated Temperatures, Materials and Structures 37 (4), 218-236.

[5] Mindeguia J-C., Hager I., Pimienta P., Carre H., La Borderie C. (2013), Parametrical study of transient thermal strain of ordinary and high performance concrete, Cement and Concrete Research 48, 40-52.

[6] Nechnech W., Meftah F., Reynouard J.M. (2002), An elasto-plastic damage model for plain concrete subjected to high temperatures, Engineering Structures 24 (5), 597-611.

[7] Sellier A., Multon S., Buffo-Lacarriere L., Vidal T., Bourbon X., Camps G. (2016), Concrete creep modelling for structural application: non-linearity, multi-axiality, hydration, temperature and drying effects, Cement and Concrete Research 79, 301-315.

[8] Sellier A., Buffo-Lacarriere L. (2009), Toward a simple and unified modeling of basic creep shrinkage and drying creep for concrete, European Journal of Environmental and Civil Engineering 10, 1161-1182.

[9] Fahmi H.M., Polivka M., Bresler B. (1972), Effects of sustained and cyclic elevated temperature on creep of concrete, Cement and Concrete Research 2 (5), 591-606.

[10] Cagnon H., Vidal T., Sellier A., Bourbon X., Camps G. (2018), Transient thermal deformation of high performance concrete in the range 20°C-40°C, under review Cement and Concrete Research.

[11] Khoury G.A., Grainger B.N., Sullivan P.J.E. (1985): Transient thermal strain of concrete: literature review, conditions within specimen and behaviour of individual constituents, Magazine of Concrete Research 37 (132), 131-44.

[12] Hansen T.C., Eriksson L. (1966), Temperature Change Effect on Behavior of Cement Paste, Mortar, and Concrete Under Load, Journal Proceedings 63 (4), 489-504.

[13] Parrot, L.J. (1974), Lateral strains in hardened cement paste under short and long-term loading, Magazine of Concrete Research 26 (89), 198-202.

[14] Torrenti J.M. (2017), Basic creep of concrete-coupling between high stresses and elevated temperatures, European Journal of Environmental and Civil Engineering, 1-10.

[15] Bažant Z.P., Kaplan M.F. (1996), Concrete at high temperatures: material properties and mathematical models, Longman Concrete design and construction series, 412-424.

[16] Bažant Z.P., Hauggaard A.B., Baweja S., Ulm F-J. (1997), Microprestress-solidification theory for concrete creep. I. Aging and drying effect, Journal of Engineering Mechanics, 123 (11), 1188-1194.

[17] Bažant Z.P., Cusatis G., Cedolin L. (2004), Temperature Effect on Concrete Creep Modeled by Microprestress-Solidification Theory, Journal of Engineering Mechanics 130 (6), 691-99.

[18] Schneider U. (1988), Concrete at high temperature-A general review, Fire Safety Journal 13 (1), 55-68.

[19] Anderberg Y., Theandersson S. (1976), Stress and deformation characteristics of concrete at high temperatures: experimental investigation and material behavior model, Lund Institute of Technology 54, 1-84.

[20] Benboudjema F., Meftah F., Torrenti J.M. (2005), Interaction between drying, shrinkage, creep and cracking phenomena in concrete, Engineering Structure 27, 239-250.

[21] Ladaoui W., Vidal T., Sellier A., Bourbon X. (2011), Effect of a temperature change from 20 to 50°C on the basic creep of HPC and HPFRC, Materials and Structures 44 (44), 1629-1639.

[22] Ladaoui W., Vidal T., Sellier A., Bourbon X. (2013), Analysis of interactions between damage and basic creep of HPC and HPFRC heated between 20 and 80°C, Materials and Structures 46 (1-2), 13-23.

[23] Vlahinić I., Thomas J.J., Jennings H.M., Andrade J.E. (2012), Transient creep effects and the lubricating power of water in materials ranging from paper to concrete and Kevlar, Journal of the Mechanics and Physics of Solids 60, 1350-1362.

[24] Jennings H.M. (2004), Colloid model of C−S−H and implications to the problem of creep and shrinkage, Materials and Structures 37 (1), 59-70.

[25] Ulm F.-J., Constantinides G., Heukamp F.H. (2004), Is concrete a poromechanics material? – A multiscale investigation of poroelastic properties, Materials and Structures 37, 43-58.

[26] Powers T.C. (1968), The thermodynamics of volume change and creep, Materials and Structures, 1(6), 487-507.

[27] Jennings H.M. (2008), Refinements to colloid model of C-S-H in cement: CM-II, Cement and Concrete Research 38 (3), 275-89.

[28] Vandamme M., Ulm F-J. (2009), Nanogranular Origin of Concrete Creep, Proceedings of the National Academy of Sciences 106 (26), 10552-57.

[29] Mensi R., Acker P., Attolou A. (1988), Séchage du béton: analyse et modélisation, Materials and structures 21 (1), 3-12.

[30] Chhun P. (2017), Modélisation du comportement thermo-hydro-chemo-mécanique des enceintes de confinement nucléaire en béton armé-précontraint, PhD Thesis – Université Paul Sabatier Toulouse, France.

[31] Tanaka M., Girard G., Davis R., Peuto A., Bignell N. (2001), Recommended Table for the Density of Water between 0 °C and 40 °C Based on Recent Experimental Reports, Metrologia 38 (4), 301-309.